OPEN ACCESS
Journal of Innovative Optical Health Sciences
2150019 (12 pages)

DOI: 10.1142/S179354582150019X

Long-term changes in mandibular bone microchemical quality after radiation therapy and underlying systemic malignancy: A pilot study

A. Palander[*,**], H. Dekker[†], M. Hyvärinen[*], L. Rieppo[‡], I. Lyijynen[§,‖], E. A. J. M. Schulten[†], C. M. Ten Bruggenkate[†], A. Koistinen[§], A. Kullaa[*,¶] and M. J. Turunen[§,‖]

[*]*Institute of Dentistry, University of Eastern Finland*
P.O. Box 1627, 70211 Kuopio, Finland

[†]*Department of Oral and Maxillofacial Surgery/Oral Pathology*
Amsterdam University Medical Centers and Academic Centre for Dentistry Amsterdam (ACTA)
Vrije Universiteit Amsterdam
De Boelelaan 1117 1081 HV Amsterdam, The Netherlands

[‡]*Research Unit of Medical Imaging*
Physics and Technology, University of Oulu
P.O. Box 5000 FI-90014 University of Oulu, Finland

[§]*SIB Labs, University of Eastern Finland*
P.O. Box 1627, 70211 Kuopio, Finland

[¶]*Educational Dental Clinic, Kuopio University Hospital*
P.O. Box 1627, 70211 Kuopio, Finland

[‖]*Department of Applied Physics, University of Eastern Finland*
P.O. Box 1627, 70211 Kuopio, Finland
[**]*anni.palander@uef.fi; anni.palander@tuni.fi*

Received 13 November 2020
Accepted 3 June 2021
Published 7 July 2021

Radiation therapy (RT) is a treatment option for head and neck cancer (HNC), but 2% of RT patients may experience damage to the jawbone, resulting in osteoradionecrosis (ORN). The ORN can manifest years after RT exposure. Changes in the local microchemical bone quality prior to the clinical manifestation of ORN could play a key role in ORN pathogenesis. Chemical bone quality can be analyzed using Fourier transform infrared spectroscopy (FTIR), that is applied to examine the effects of cancer, chemotherapy, and RT on the quality of human mandibular bone. Cortical mandibular bone samples were harvested from dental implant beds of

[**]Corresponding author.

23 individuals, i.e., patients with surgically and radiotherapeutically treated HNC (RT-HNC, $n = 7$), surgically and radiochemotherapeutically treated HNC (CH-RT-HNC, $n = 3$), only surgically treated HNC (SRG-HNC, $n = 4$), and healthy controls ($n = 9$). Infrared spectra were acquired from two representative regions of interest in cortical mandibular bone. Spectral parameters, i.e., mineral-to-matrix ratio (MM), carbonate-to-matrix ratio (CM), carbonate-to-phosphate ratio (CP), collagen maturity (cross-linking), crystallinity, acid phosphate substitution (APS), and advanced glycation end products (AGEs), were analyzed for each sample. Amide I region of the CH-RT-HNC group differed from the control group in cluster analysis ($p = 0.02$). Apart from a minor variation trend in collagen maturity ($p = 0.07$), there were no other significant differences between the groups. Thus, the effect of radiochemotherapy on mandibular bone composition should be further investigated. In future trials, this study design is potential when the effects of the cancer burden and different HNC treatment modalities on jawbone composition are studied, in order to reveal ORN pathogenesis.

Keywords: Mandibular bone; radiation therapy; Fourier transform infrared spectroscopy.

1. Introduction

In patients with head and neck cancer (HNC), the jawbones are often secondarily affected by radiation therapy (RT), which is used as an adjunctive cancer treatment in conjunction with surgery and/or chemotherapy. Radiation can cause irreversible damage to bone tissue; in its extreme form, this is called osteoradionecrosis (ORN). According to the recently postulated fibroatrophic theory, the bone tissue goes through three phases after RT: a pre-fibrotic phase, a constitutive organized phase, and a late fibroatrophic phase. The late stage can occur even decades after the initial exposure and is also referred to as radiation-induced fibrosis (RIF).[1] These irradiated areas remain fragile and in 2% of the RT patients, they can develop into regions of local ischemia and spontaneous ORN. The incidence of ORN rises further to 7% in cases of a surgical trauma.[2] Irradiation also increases the risk ratio of dental implant loss by approximately 2.7–6-fold, depending on the implant site.[3] However, the molecular pathways leading to ORN and dental implant loss processes are not clear. One central factor in the development of RIF could be microchemical changes occurring in bone quality. The term bone quality refers to the capacity of bone tissue to resist strain and fracture. The main quality-contributing factors are the bone's microarchitecture, accumulated microscopic-level damage, the quality of collagen, the mineral quality and content, the size and perfection of mineral crystals, and the rate of bone turnover.[4]

This microchemical bone quality can be investigated using Fourier transform infrared spectroscopy (FTIR) which is a technique that detects molecular vibrations of tissues, reflecting their molecular composition. Hence, the potential changes in the quality of bone inorganic and organic components after RT can be detected by FTIR.[5] Bone is a composite tissue consisting of both inorganic and organic components and the mineral-to-matrix ratio (MM) reflects the ratio between these inorganic and organic phases. The inorganic material consists mainly of hydroxyapatite [$(Ca_{10}(PO_4)_6(OH)_2)$; HA][6] within which the hydroxyl or phosphate groups can be substituted, mostly with carbonate, referring to type A or type B substitutions, respectively.[7] The total carbonate substitution, encompassing types A, B and labile carbonate, can be estimated from the carbonate-to-phosphate ratio (CP).[7] The carbonate content can be evaluated from the carbonate-to-matrix ratio (CM). Generally, the extent of carbonation increases with time in synthetic HA, although *in vivo*, the results are more controversial.[8] In *in-vivo* studies, the carbonate content has also been shown to be high in the early stages of mineralization.[9] Thus, an assessment of carbonation is important because carbonate is considered as a cumulative impurity that may increase bone brittleness.[10] Another factor contributing to mineral quality is mineral maturity, i.e., the size and perfection of the HA crystals, often determined by the crystallinity parameter in FTIR.[10,11] Bone tissue is also being constantly remodeled, and new bone formation can be assessed by the amount of acid phosphate substitution (APS) in FTIR.[11,12] The organic bone matrix consists mainly of type I collagen; in the FTIR

spectrum, the amide I peak represents the collagen content. FTIR can also assess the maturity of collagen based on estimates of collagen enzymatic cross-linking.[13] In contrast, the presence of nonenzymatic cross-links can disturb the composition and mechanical properties of the organic matrix.[14] One type of nonenzymatic cross-linking that can be estimated from the FTIR spectrum is the accumulation of so-called advanced glycation end products (AGEs)[15]; these have been found to increase in bone tissue due to irradiation.[16,17]

Previously, FTIR has been applied to examine irradiation-induced changes in living bone only in mouse tibias.[18,19] The tibias were irradiated with 5 Gy (gray) and a decline in mineral content was observed in the trabecular bone at 10 days. At eight weeks, however, the extent of mineralization had increased. In contrast, cortical tibial bone showed no significant compositional changes during the observation period.[18] Another study has also examined mouse tibial reactions with attenuated total reflectance Fourier transform infrared spectroscopy (ATR-FTIR). In that study, collagen maturity was significantly lower 30 days after 30-Gy irradiation, but the difference was no longer observable after 60 days. However, crystallinity increased 60 days after RT.[19] Nonetheless, it is evident that the reactions are not directly comparable between tibial bone and mandibular bone[20] or between murine bone and human bone.[21] The follow-up times in the mouse studies were only two months, which is not long enough to provide information about the long-term effects of RT. Clarifying the long-term changes in mandibular bone would be extremely important, as ORN can develop even several years after RT. Furthermore, animal experiments have not considered the possible effects of chemotherapy as well as preexisting cancer on bone quality.

In humans, no FTIR studies have been conducted on irradiated jawbone. However, a few investigators have applied other techniques to examine RIF in this tissue. Dekker *et al.*[22] studied vascular changes with microcomputed tomography; they reported that irradiation decreased vascular density, vascular area fraction, and small vessel number with the changes being more significant when the local dose exceeded 50 Gy. Two previous publications described the application of Raman spectroscopy in the evaluation of the effects of RT.[23,24] While the study by Singh *et al.*[24] also considered the effect of cancer, it did not assess the impact of chemotherapy. In that study, the mineral component in the bone of cancer patients was diminished (decreased MM, phosphate content, and crystallinity) and there was evidence of an increased accumulation of impurities (increased CP) in comparison to both irradiated patients and control but between the two latter groups, no significant differences could be detected.[24] Lakshmi *et al.*[23] described a deterioration in the lipid content and mineral composition of irradiated subjects. These studies on human subjects, however, did not consider the individual effects of cancer, chemotherapy, and RT on the properties of the jawbone.

The aim of this pilot study is to evaluate the long-term compositional/chemical changes attributable to RIF in human mandibular bone tissue that do not exhibit clinical signs of ORN. Furthermore, this study aims to distinguish whether the possible chemical changes in bone are influenced by RT, chemotherapy, or the primary tumor with no clinical signs of bone invasion.

2. Materials and Methods

We evaluated 23 mandibular cortical bone samples that were harvested from the lower canine dental implant beds of 23 implant rehabilitation patients in the Department of Oral and Maxillofacial Surgery, Amsterdam University Medical Centers (UMC), Vrije University Medical Center (VUmc), The Netherlands. The biopsy material consisted of excess waste tissue produced during standard implant therapy that was indicated as a part of standard oral rehabilitation protocol after head and neck cancer treatment in patients with a history of HNC. The patients in the first study group [surgically and radiotherapeutically treated HNC (RT-HNC)] had HNC that was treated with surgery and radiotherapy ($n = 7$; five males, two females, age range: 51–74 years). The second group [surgically and radiochemotherapeutically treated HNC (CH-RT-HNC)] consisted of HNC patients treated with surgery and radiochemotherapy ($n = 3$; two males, one female, age range: 54–69 years). In this group, cisplatinum (100 mg/m^2 per day) was administered in three cycles (on days 1, 22, and 43) concomitant with RT. All subjects in the RT-HNC and CH-RT-HNC groups had received hyperbaric oxygen (HBO) treatment before the biopsy according to the standard protocol in Amsterdam UMC, VUmc. The third study group [surgically treated HNC (SRG-

HNC); $n = 4$; four males, age range: 57–79 years] consisted of patients who received only surgical treatment of their tumor. This group was investigated to reveal the possible systemic metabolic changes that the cancer itself could have inflicted on bone tissue. The tumors in all three groups showed no evidence of bone invasion. Finally, the fourth group consisted of healthy control patients ($n = 9$; four males, five females, age range: 51–70 years), that had standard dental implant therapy for masticatory function improvement. The patients in this study had no history of bone-affecting illnesses, current or previous bone-affecting medications (e.g., a history of bisphosphonate use or systemic immunosuppressive medication), underlying malignancies, or impaired bone metabolism (e.g., hyperparathyroidism, osteomalacia). Cardiovascular comorbidities were acceptable in the RT-HNC and CH-RT-HNC groups. The included patients had normal blood levels of calcium, phosphate, parathyroid hormone, and HbA1c three months before sample harvesting. All patients had given their consent to participate in the study and the work was approved by the ethical committees in compliance with the Helsinki Declaration (Medisch Ethische Toetsingscommissie, Amsterdam UMC, location VUmc, Amsterdam, The Netherlands, 2011/220; and the Research Ethics Committee of Northern Savo Hospital District, 754/2018).

2.1. *Sample harvesting and preparation*

Bone biopsies were harvested from dental implant beds in the mandibular canine region with a 3.5-mm-diameter trephine drill (Straumann® Dental Implant System; Straumann Holding AG, Basel, Switzerland) to a depth of 10 mm or 12 mm. In the control group, the surgical procedure was performed under local anesthesia and in the RT-HNC, CH-RT-HNC, and SRG-HNC groups under general anesthesia. Table 1 presents the timing from RT to biopsy in the RT-HNC and CH-RT-HNC groups and the timing from tumor surgery to biopsy in the SRG-HNC group. Total RT doses targeted at the patients in RT-HNC and CH-RT-HNC groups were retrospectively evaluated from RT plans.

All specimens were fixed and dehydrated with increasing concentrations of ethanol and embedded in Poly-methyl methacrylate (PMMA; Merck KGaA). A microtome (Polycut S; Reichert-Jung, Wien, Austria) was used for cutting the 3-μm-thick sections for FTIR and the 10-μm-thick sections for bright field microscopy. The 3-μm-thin sections were placed on BaF_2 windows, whereas the 10-μm-thick

Table 1. Background variables and significant differences (*) of experimental groups compared to control group by Mann–Whitney U-test and Fischer's exact test (significance level of $p \leq 0.05$).

	Control ($n = 9$)	SRG-HNC ($n = 4$)	RT-HNC ($n = 7$)	CH-RT-HNC ($n = 3$)
Age in years, median (IQR)	65 (58–67) reference	68 (60–77) $p = 0.60$	63 (62–64) $p = 0.68$	60 (57–65) $p = 0.73$
Females, number of patients (%)	5 (55.6%) reference	0 (0%) $p = 0.11$	2 (28.6%) $p = 0.36$	1 (33.3%) $p = 1$
Comorbidities,[a] number of patients (%)	0 (0%) reference	0 (0%) $p = 1$	6 (85.7%) $p = 0.001^*$	2 (66.7%) $p = 0.05^*$
Smoking at the time of biopsy, number of patients (%)	0 (0%) reference	2 (50%) $p = 0.08$	3 (42.9%) $p = 0.06$	1 (33.3%) $p = 0.25$
Alcohol use at the time of biopsy, number of patients (%)	3 (33.3%) reference	3 (75%) $p = 0.27$	5 (71.4%) $p = 0.32$	0 (0%) $p = 0.51$
Time interval between RT and biopsy, median (IQR)		1 year and 1 month (11.5 months–1 year and 2.5 months)[b]	16 years and 6 months (8 years and 1 month–16 years and 10.5 months) reference	7 years and 1 month (7 years–8 years and 8.5 months) $p = 0.38$
RT total dose in Gy, median (IQR)			62.5 (62.3–68) reference	70 (55–70) $p = 0.83$

Notes: [a]Cardiovascular comorbidities. [b]Timing from tumor surgery to biopsy.

sections were stained with Masson–Goldner trichrome (MG) and fixed on glass microscope slides.

2.2. *FTIR spectroscopic imaging*

The MG-stained sections were imaged with a bright field microscope (Zeiss AxioImager M2; Carl Zeiss GmbH, Jena, Germany) for sample overview and region of interest (ROI) selection for FTIR spectroscopic imaging. A schematic image of sample overview is presented in Fig. 1. Two 200 μm × 200μm ROIs distant from each other and of representative dense cortical bone were selected from each specimen and imaged with FTIR imaging microscopes (Perkin Elmer Spotlight 300 or Agilent Cary 620/670). Depending on the device, the imaging was performed in the transmission mode with a wavenumber range of 2000–800 cm^{-1} or 3800–800 cm^{-1} using a pixel size of 6.25 μm or 5.50 μm, respectively. The spectral resolution for each sample was 4 cm^{-1} with eight repeated scans. A reference spectrum from pure PMMA was also collected from each sample. A background scan was performed on a clean BaF_2 window with the same imaging parameters but with an average of 75 scans.

2.3. *Data analysis*

All spectra were trimmed to the wavenumber range of 2000–800 cm^{-1}. For each measurement region, spectra that were not collected from bone (e.g., hole at the section with only window and close-to-zero absorbance) or showed any full absorbance (i.e., saturation of the phosphate peak) were excluded.

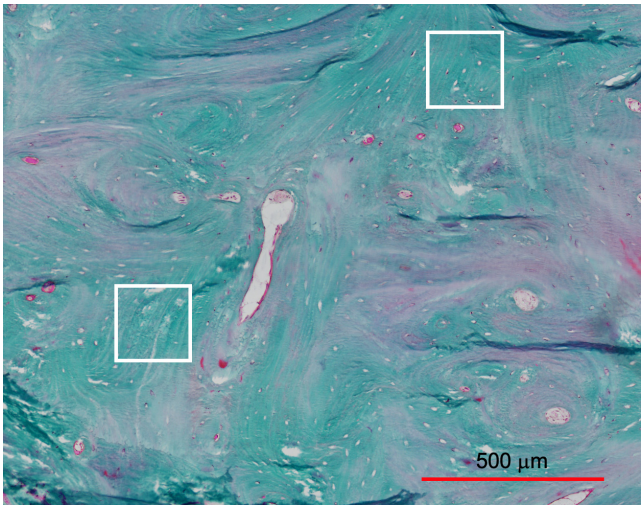

Fig. 1. Schematic image of the FTIR measurement points.

The included spectra were averaged per sample to obtain a spectrum with high signal-to-noise ratio. The PMMA reference spectrum (section-specific) was mathematically subtracted from each averaged bone spectrum.[25] In short, the bone spectrum was normalized to the PMMA spectrum using the intensity at a wavenumber of 1730 cm^{-1}. Subsequently, the PMMA spectrum was subtracted from the normalized bone spectrum and the bone spectrum was scaled back to the original using the inverse of the scaling factor from the initial normalization. Figure 2 shows an example of bone infrared absorption spectrum after PMMA subtraction. After PMMA subtraction, integrated areas of absorbance peaks at 1200–900 cm^{-1} for phosphate, 890–850 cm^{-1} for carbonate, and 1720–1585 cm^{-1} for amide I were calculated from each bone absorbance spectrum. Prior to integration, each peak was linearly baseline-corrected using the same above-mentioned basepoints. From these peaks, the following typical compositional parameters of bone were derived, i.e., MM, CP, and CM ratios.[11] In addition, from the bone spectra intensity ratios, collagen maturity (1660 cm^{-1}/1690 cm^{-1}, which is related to collagen cross-linking),[13] crystallinity (1030 cm^{-1}/1020 cm^{-1}),[11] and acid phosphate substitution (1127 cm^{-1}/1096 cm^{-1})[11,12] were determined. For these parameters, intensity ratios have been routinely used by different study groups in the comparison of the compositional properties of bone.[11,26] Peak fitting of the mean spectrum of each ROI was performed to estimate the ratio of 1678 cm^{-1}/1692 cm^{-1} that is descriptive for AGEs. Peak fitting was done in similarly as in the previous publication, i.e., the amide I band was

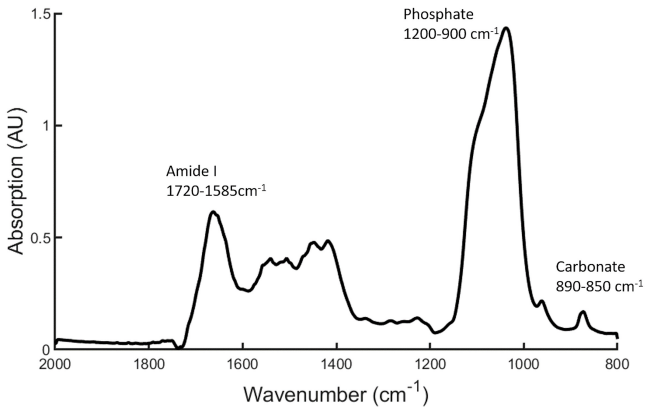

Fig. 2. Infrared absorption spectrum of bone tissue after baseline correction and PMMA subtraction.

fitted with seven Gaussian subbands (1702, 1694, 1678, 1661, 1645, 1630, and 1610 cm^{-1}).[15] All spectral analyses were performed with custom-made MATLAB scripts (R2016b; The MathWorks, Inc., MA).

2.4. *Statistical analyses*

Statistical analyses were performed between the study groups (RT-HNC, $n = 7$; CH-RT-HNC, $n = 3$; SRG-HNC, $n = 4$; and control, $n = 9$). Median values and inter-quartile ranges (IQRs) of each group were calculated due to their skewed distribution, with 95% confidence intervals. Values were normalized to the control group (dividing by control) in each category. All statistical tests between groups were carried out using Mann–Whitney U-test or Kruskal–Wallis test for continuous variables and Fischer's exact test for categorical background variables (IBM SPSS Statistics 26). The p-values of $p \leq 0.05$ were considered statistically significant. Additionally, a Fuzzy C-means (FCM) cluster analysis was used to compare the spectral profiles of the samples.[27] Two reference average spectra, that were least correlated with each other, were calculated from the full dataset. Then, the average spectrum of each sample was compared with these reference spectra and categorized into two clusters (red or green) based on the best match with the reference spectra. Brightness of the cluster color (between 0 and 1) in Fig. 4 represents a higher probability of belonging to certain cluster. The FCM cluster analysis was run for four different regions of the IR spectrum: amide (A, 1710–1350 cm^{-1}, consisting of amide I and II regions), amide I (AI, 1710–1610 cm^{-1}), carbonate (C, 910–840 cm^{-1}), and phosphate (P, 1180–975 cm^{-1}). Before clustering, the spectra were normalized to the maximum of the spectra in each region in order to base the clustering on the spectral shape rather than intensity variations (which can be affected by biological variation as well as section thickness). After clustering, statistical tests between groups were carried out using Fischer's exact test. Furthermore, a principal component analysis (PCA) was performed on the mean spectra at the fingerprint region of 1800–800 cm^{-1} after vector normalization (MATLAB). The scores of the two first principal components were investigated to determine whether the studied sample groups formed separate clusters or whether there are potential outliers in study groups.

3. Results

The background variables of the groups are presented in Table 1. In the RT-HNC and CH-RT-HNC groups, there were significantly more comorbidities than in the other groups. Six patients in the RT-HNC group and two patients in the CH-RT-HNC group were suffering from cardiovascular diseases. With respect to all other parameters, however, the groups were statistically homogeneous. Median timing from surgery to biopsy in the SRG-HNC group (one year and one month) was not compared to time intervals of RT to biopsy because the comparison would have been inappropriate.

The SRG-HNC group was investigated to reveal the probable effects that HNC alone could have inflicted on bone quality. However, the SRG-HNC group did not show any statistically significant differences and sample-to-sample variation was considerable (Fig. 3). Also, the cluster analysis did not reveal differences between the SRG-HNC group compared to other study groups (Fig. 4). In PCA the control group appeared most uniform, whereas other study groups showed more variation (Fig. 5). The SRG-HNC group had one potential outlier, but other subjects in the SRG-HNC group were not separable from other study groups.

In the RT-HNC group, none of the patients presented with clinical ORN. The chemical composition across all FTIR parameters in the RT-HNC group was not statistically different compared to other study groups. Group median values and IQRs are presented in Fig. 3. The deviation of the spectral features in the RT-HNC was slightly more scattered than in the spectra from the control group, but the spectra were relatively uniform as there was major overlap observed in PCA (Fig. 5). Neither did cluster analysis separate the RT-HNC group from other groups.

The CH-RT-HNC group was used to assess the effects of both RT and adjuvant chemotherapy. In the CH-RT-HNC group none of the patients presented with clinical ORN. In cluster analysis, the amide I region was significantly different between the CH-RT-HNC and the control group ($p = 0.02$) (Fig. 4). Similar trend ($p = 0.07$) was also seen in

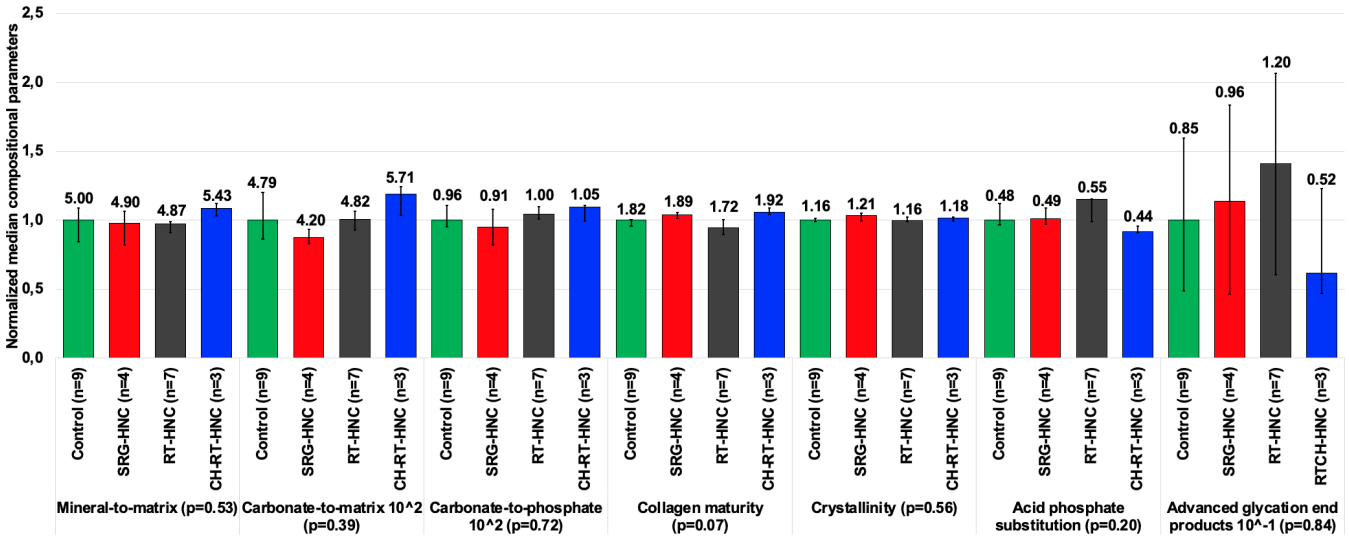

Fig. 3. FTIR parameters (medians and IQRs normalized to control level, absolute values above bars). There were no significant differences between study groups by Kruskal–Wallis test (significance level of $p \leq 0.05$).

collagen maturity, that was highest in the CH-RT-HNC group (Fig. 3). On the other hand, there was overlap in confidence intervals of collagen maturity across all groups and the CH-RT-HNC group also overlapped with other groups in PCA analysis (Fig. 5).

4. Discussion

The aim of this study was to investigate the changes in bone chemical quality due to the systemic HNC cancer burden, chemotherapy, and RT. The results suggest that combined radiochemotherapy may

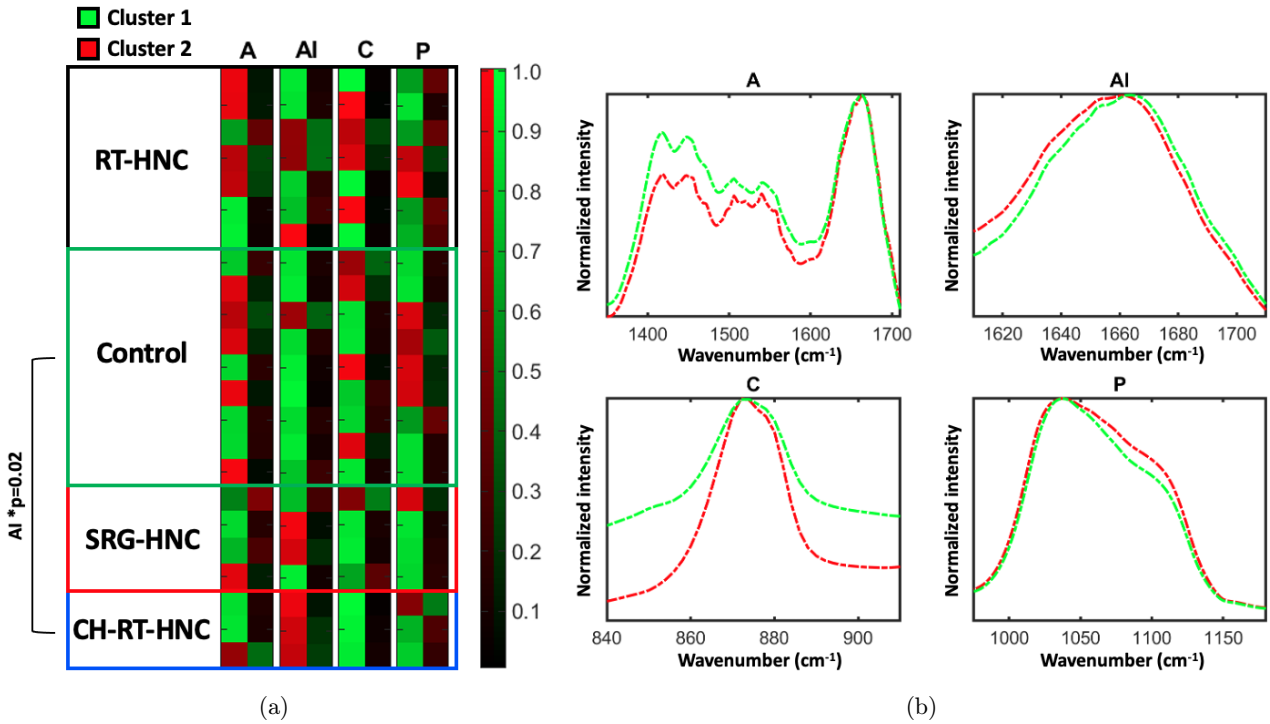

(a) (b)

Fig. 4. (a) Samples categorized into clusters based on amide (A), amide I (AI), carbonate (C), and phosphate (P) regions of the (b) averaged and normalized IR spectra clusters. For each spectral region, primary (left column) and secondary (right column) clusters and the probability of each sample belonging to each cluster [0 1] are plotted using color maps. Significant differences (*) between study groups by Fischer's exact test (significance level of $p \leq 0.05$).

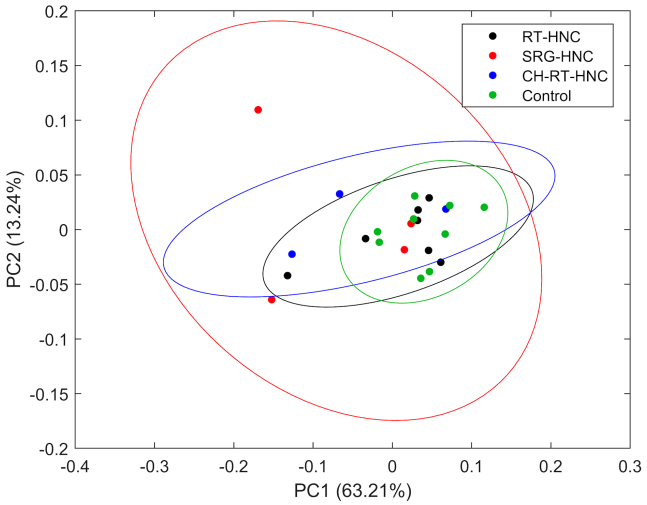

Fig. 5. Principal component analysis of IR spectra between the groups. Lines represent CI of 95%.

have an effect on bone organic component, as revealed from the altered amide I region of the CH-RT-HNC group in the cluster analysis and a trend of increased collagen cross-linking. Biologically, the changes in collagen secondary structure (i.e., denaturation, hydrogen bonding, and cross-linking) affect the amide regions in FTIR spectra.[28,29] From a technical point of view the altered amide I region in cluster analysis may reflect the variation of its subbands 1660 cm^{-1} and 1690 cm^{-1} that are used to analyze collagen maturation (cross-links).[30] However, it is important to note that the small number of samples in this study may have reduced the statistical power or, in turn, increased the risk of bias. Larger sample sizes are required in future trials before solid conclusions can be made.

The processes of bone responses initially attributable to the cancer burden and thereafter to chemotherapy and the irradiation damage are very complex but may be better understood clinically if the events are placed on a timeline, as this study presented. First, the systemic burden of cancer did not seem to alter bone composition. None of the patients in the SRG-HNC group had received chemotherapy and had no general medications or comorbidities, which reduces the risk of bias. In contrast to this study, a previous study with Raman spectroscopy reported systemic changes in bone composition as a result of a cancer that had not caused clinical evidence of affecting the bone.[24] Curi *et al.*[31] also used cancer patients as a control group in their histomorphometric study of actual ORN, but they did not compare between healthy subjects and the patients with cancer. The hypothetical disturbance in bone composition could stem from increased metabolic and/or inflammatory activity in the tumor site, which could be mediated through several growth and inflammatory factors secreted by cancer cells.[32] However, it is not known whether the possible effects on bone would be affected by individual variation, changes in the tumor microenvironment, the function of the immune system, the presence of inflammation, or due to a putative pre-metastatic niche, where the tumor prepares potential organs for metastases.[33] Nevertheless, when FTIR has examined actual clinical bone metastases, there have been clear signs of suppression of all mineral parameters,[34] hence the bone samples in this study cannot be defined as metastatic. Furthermore, all the biopsies in this study were taken at approximately one year after tumor surgery, suggesting that the probable effects of cancer on bone microstructure may not be long-lasting. The tumor staging affects the selected treatment protocol and it would be of interest to examine whether higher stages would correlate with greater chemical disturbances in mandibular bone. Unfortunately, stage-dependency could not be investigated in this study due to insufficient patient data. Most reliable data could be acquired if biopsies were taken from patients both pre- and post-operatively as this would make it possible to demonstrate changes in bone quality within the same individual. However, this would result in additional harm and tissue loss to the patients.

The long-term effects of surgical removal of the tumor and subsequent adjuvant RT were preliminarily evaluated in this pilot study. There were no statistically significant changes due to RT compared to control or surgically treated patients, but the effect of small sample size on statistical power should be considered. The median observation period of 16 years and 6 months was considerably long, which may give the tissue time to replace the probable damage. However, it remains as a question how the ORN could manifest decades after RT exposure, if bone repair processes would be functional. It has been proposed that as a result of RT, the function of osteoblasts is diminished and this could lead to impaired collagen metabolism and bone turnover.[35,36] In a previous Raman spectroscopy study conducted in mice, it was also proposed that elevated amounts of pathological collagen

cross-links would slow down the remodeling process.[37] This kind of slowing down of metabolic activity was discussed also in a Raman study performed in human subjects by Lakshmi *et al.*[23] They observed a deterioration in the lipid content (cellular and bone marrow) and mineral composition of irradiated subjects. Evidence of organic matrix defects was also detected in mouse experiments reported by Gong *et al.*[37] and Limirio *et al.*[19] Accordingly, RT could lead to formation of a deranged collagen scaffold, that subsequently would alter mineral and other tissue properties.[37] There seems to be a discrepancy between mouse and human studies, as most mouse studies generally have shown a deterioration in several bone quality parameters.[18,19,37] This study, however, detected no significant differences in collagen maturity between the RT group and the control group. This discrepancy could stem from the shorter observation period utilized in animal studies. One noteworthy aspect here is also that animal studies have applied RT on healthy bone, whereas human studies deliver RT as cancer treatment, where the presence of cancer and chemotherapy are confounding factors. On the other hand, in the mouse study conducted by Green *et al.*,[18] there were no significant changes in tibial cortical bone. Our study also focused on cortical bone, which can explain the lack of changes in the RT group. The effect of the radiation dose is also an issue worth considering, as doses over 50 Gy are thought to be critical for the increased ORN risk.[38] In both the RT-HNC and CH-RT-HNC groups, the total doses were higher than 50 Gy, suggesting that the results of this study may be applicable only when evaluating high-dose effects. However, the local dose at the biopsy site may differ from the total dose. Unfortunately, local dose was unavailable for too many subjects in this study for reliable analysis.

Patients that had received radiochemotherapy (CH-RT-HNC group) presented slightly higher collagen maturity and significantly different amide I region compared to the control group. As previously discussed, this might be due to changes in collagen secondary structure. However, the interpretation must be conducted with caution, because of the small sample size in the CH-RT-HNC group. Previously in dogs, chemotherapy has temporarily suppressed bone metabolic functions.[39] However, the focus of this study was on long-term changes, while bone tissue had potentially recovered from medical suppression. Of course, as this study suggests, the combination of both RT and chemotherapy on bone can be unexpectable and short-term effects of radiochemotherapy should be assessed in the future. Again, it is interesting to place the processes on a timeline as the comparison between cancer burden, chemotherapy, and RT exposures was the focus of this study. In humans, it is challenging to recognize the effect of each exposure separately, and such a study design would not be ethical to conduct on humans.

In this study, some of the compositional parameters are calculated as intensity ratios from the spectra. These ratios may be susceptible to changes in the peak shifting and signal-to-noise ratio, which can be considered as a limitation in this study. A more sophisticated method used in the determination of these compositional parameters is peak-fitting, which can also be considered as a golden standard of the analysis.[11,13,26,40,41] However, there are considerable limitations also in the peak-fitting approach. It is a very sensible method that can lead to many mistakes from a mathematical point of view. Since the direct intensity ratios have been used routinely in the FTIR bone research,[12,42–45] despite its limitations, it was used also in this study. To reduce the error posed by these factors, we calculated an average spectrum for each measurement area to increase the signal-to-noise ratio of the analyzed spectrum, and to decrease the possible errors due to shifts in the peak positions. When looking at the transmission spectra of the samples, the phosphate peak region had close to zero values, typical for even thin bone sections, which could be indication a moderate risk of saturation in some wavelengths. However, for each sample a slope in the phosphate peak close to minimum transmission was observed deducting the doubts related to the possible saturation and increasing the reliability of the data.

In this study, the RT-HNC and CH-RT-HNC groups had significantly more cardiovascular comorbidities than the other study groups. The cardiovascular comorbidities in the RT-HNC group, however, are not primarily bone-affecting diseases, hence their effect on bone could be considered as minimal. Other challenges in this study were also related to sample variability and the small sample size. HNCs are predominant in males, which caused some imbalance in the groups' gender frequencies. The difference in mandibular cortical bone quality

between males and females has not been studied by FTIR, but within our healthy control group, the differences in bone quality parameters between males and females were not statistically significant even though it is known that in women, menopause affects bone quality.[46] Therefore, all the female subjects in this study were selected as being of postmenopausal age (over 50 years), which improves sample homogeneity. On the other hand, the results may not apply to younger patients, as FTIR spectroscopic compositional parameters in bones do change as a function of age.[47,48]

5. Conclusions

This pilot study examined the probable microchemical changes in mandibular bone tissue after exposure first to the burden of cancer and thereafter to the curative interventions of chemotherapy and radiotherapy. There were no significant differences in bone composition in the long term. However, the baseline effects caused by the primary tumor and chemotherapy should be considered when assessing RT-induced changes in future trials in both short and long terms. With larger sample sizes the current study design has the potential to reveal the more exact effects of these individual factors. Further studies with larger sample sizes will be needed to explore the role of bone chemical quality in the pathogenesis of RIF and ORN.

Conflict of Interest

The authors declare that there are no conflicts of interest relevant to this paper.

Acknowledgments

The authors acknowledge Ritva Savolainen for help with sample preparation, Dr. Laure Fauch for Fig. 1, and Dr. Ewen MacDonald for English language editing.

References

1. S. Delanian, J. L. Lefaix, "The radiation-induced fibroatrophic process: therapeutic perspective via the antioxidant pathway," *Radiother. Oncol.* **73**, 119–131 (2004).
2. S. Nabil, N. Samman, "Incidence and prevention of osteoradionecrosis after dental extraction in irradiated patients: a systematic review," *Int. J. Oral Maxillofac. Surg.* **40**, 229–243 (2011).
3. L. Chambrone, J. Mandia, Jr., J. A. Shibli, G. A. Romito, M. Abrahao, "Dental implants installed in irradiated jaws: A systematic review," *J. Dent. Res.* **92**, 119S–130S (2013).
4. H. Fonseca, D. Moreira-Gonçalves, H. J. A. Coriolano, J. A. Duarte, "Bone quality: The determinants of bone strength and fragility," *Sports Med.* **44**, 37–53 (2014).
5. D. Chappard, M. F. Baslé, E. Legrand, M. Audran, "New laboratory tools in the assessment of bone quality," *Osteoporos. Int.* **22**, 2225–2240 (2011).
6. E. A. B. Hughes, T. E. Robinson, D. B. Bassett, S. C. Cox, L. M. Grover, "Critical and diverse roles of phosphates in human bone formation," *J. Mater. Chem. B* **21**, 7460–7470 (2019).
7. C. Rey, B. Collins, T. Goehl, I. R. Dickson, M. J. Glimcher, "The carbonate environment in bone mineral: A resolution-enhanced Fourier transform infrared spectroscopy study," *Calcif. Tissue Int.* **45**, 157–164 (1989).
8. Y. Bala, D. Farlay, G. Boivin, "Bone mineralization: from tissue to crystal in normal and pathological contexts," *Osteoporos. Int.* **24**, 2153–2166 (2013).
9. Y. Bala, D. Farlay, P. D. Delmas, P. J. Meunier, G. Boivin, "Time sequence of secondary mineralization and microhardness in cortical and cancellous bone from ewes," *Bone* **46**, 1204–1212 (2010).
10. N. Kourkoumelis, X. Zhang, Z. Lin, J. Wang, "Fourier transform infrared spectroscopy of bone tissue: Bone quality assessment in preclinical and clinical applications of osteoporosis and fragility fracture," *Clinic. Rev. Bone Miner. Metab.* **17**, 24–39 (2019).
11. A. Boskey, N. Pleshko Camacho, "FT-IR imaging of native and tissue-engineered bone and cartilage," *Biomaterials* **28**, 2465–2478 (2007).
12. L. Spevak, C. R. Flach, T. Hunter, R. Mendelsohn, A. Boskey, "Fourier transform infrared spectroscopic imaging parameters describing acid phosphate substitution in biologic hydroxyapatite," *Calcif. Tissue Int.* **92**, 418–428 (2013).
13. E. P. Paschalis, K. Verdelis, S. B. Doty, A. L. Boskey, R. Mendelsohn, M. Yamauchi, "Spectroscopic characterization of collagen cross-links in bone," *J. Bone Miner. Res.* **16**, 1821–1828 (2001).
14. M. Saito, K. Marumo, "Collagen cross-links as a determinant of bone quality: A possible explanation for bone fragility in aging, osteoporosis, and diabetes mellitus," *Osteoporos. Int.* **21**, 195–214 (2009).

15. F. Schmidt, E. Zimmermann, G. Campbell, G. Sroga, K. Püschel, M. Amling, S. Y. Tang, D. Vashishth, B. Busse, "Assessment of collagen quality associated with non-enzymatic cross-links in human bone using Fourier-transform infrared imaging," *Bone* **97**, 243–251 (2016).
16. H. D. Barth, E. A. Zimmermann, E. Schaible, S. Y. Tang, T. Alliston, R. O. Ritchie, "Characterization of the effects of X-ray irradiation on the hierarchical structure and mechanical properties of human cortical bone," *Biomaterials* **32**, 8892–8904 (2011).
17. M. E. Oest, T. A. Damron, "Focal therapeutic irradiation induces an early transient increase in bone glycation," *Radiat. Res.* **181**, 439–443 (2014).
18. D. E. Green, B. J. Adler, M. E. Chan, J. J. Lennon, A. S. Acerbo, L. M. Miller, C. T. Rubin, "Altered composition of bone as triggered by irradiation facilitates the rapid erosion of the matrix by both cellular and physicochemical processes," *PLoS ONE* **8**, e64952 (2013).
19. P. H. J. O. Limirio, P. B. F. Soares, E. T. P. Emi, C. C. A. Lopes, F. S. Rocha, J. D. Batista, G. D. Rabelo, P. Dechichi, "Ionizing radiation and bone quality: Time-dependent effects," *Radiat. Oncol.* **14**, 15 (2019).
20. M. Damek-Poprawa, S. Both, A. C. Wright, A. Maity, S. O. Akintoye, "Onset of mandible and tibia osteoradionecrosis: a comparative pilot study in the rat," *Oral Surg. Oral Med. Oral Pathol. Oral Radiol.* **115**, 201–211 (2013).
21. R. Jilka, "The relevance of mouse models for investigating age-related bone loss in humans," *J. Gerontol. A, Biol. Sci. Med. Sci.* **68**, 1209–1217 (2013).
22. H. Dekker, N. Bravenboer, D. van Dijk, E. Bloemena, D. H. F. Rietveld, C. M. Ten Bruggenkate, E. A. J. M. Schulten, "The irradiated human mandible: A quantitative study on bone vascularity," *Oral Oncol.* **87**, 126–130 (2018).
23. R. J. Lakshmi, M. Alexander, J. Kurien, K. K. Mahato, V. B. Kartha, "Osteoradionecrosis (ORN) of the mandible: A laser Raman spectroscopic study," *Appl. Spectrosc.* **57**, 1100–1116 (2003).
24. S. Singh, I. Parviainen, H. Dekker, E. Schulten, C. ten Bruggenkate, N. Bravenboer, J. J. Mikkonen, M. J. Turunen, A. P. Koistinen, A. M. Kullaa, "Raman microspectroscopy demonstrates alterations in human mandibular bone after radiotherapy," *J. Anal. Bioanal. Tech.* **6**, 1000276 (2015).
25. H. Isaksson, M. J. Turunen, L. Rieppo, S. Saarakkala, I. S. Tamminen, J. Rieppo, H. Kröger, J. S. Jurvelin, "Infrared spectroscopy indicates altered bone turnover and remodeling activity in renal osteodystrophy," *J. Bone Miner. Res.* **25**, 1360–1366 (2010).
26. E. P. Paschalis, E. DiCarlo, F. Betts, P. Sherman, R. Mendelsohn, A. L. Boskey, "FTIR microspectroscopic analysis of human osteonal bone," *Calcif. Tissue Int.* **59**, 480–487 (1996).
27. Y. Kobrina, M. J. Turunen, S. Saarakkala, J. S. Jurvelin, M. Hauta-Kasari, H. Isaksson, "Cluster analysis of infrared spectra of rabbit cortical bone samples during maturation and growth," *Analyst* **135**, 3147–3155 (2010).
28. D. Southern, G. Lutz, A. Bracilovic, P. West, M. Spevak, N. P. Camacho, S. Doty, "Histological and molecular structure characterization of annular collagen after intradiskal electrothermal annuloplasty, *HSS J.* **2**, 49–54 (2006).
29. P. A. West, M. P. G. Bostrom, P. A, Torzilli, N. P. Camacho, "Fourier transform infrared spectral analysis of degenerative cartilage: An infrared fiber optic probe and imaging study," *Appl. Spectrosc.* **58**, 376–381 (2004).
30. E. P. Paschalis, S. Gamsjaeger, D. N. Tatakis, N. Hassler, S. P. Robins, K. Klaushofer, "Fourier transform infrared spectroscopic characterization of mineralizing type I collagen enzymatic trivalent cross-links," *Calcif. Tissue Int.* **96**, 18–29 (2015).
31. M. M. Curi, C. L. Cardoso, H. G. de Lima, L. P. Kowalski, M. D. Martins, "Histopathologic and histomorphometric analysis of irradiation injury in bone and the surrounding soft tissues of the jaws," *J. Oral Maxillofac. Surg.* **74**, 190–199 (2016).
32. F. Bronner, M. C. Farach-Carson, *Bone and Cancer*, 1st Edition, Springer London, London (2009).
33. Y. Liu, X. Cao, "Characteristics and significance of the pre-metastatic niche," *Cancer Cell* **30**, 668–681 (2016).
34. D. Chappard, G. Mabilleau, C. Masson, A. Tahla, E. Legrand, "Metaplastic woven bone in bone metastases: A Fourier-transform infrared analysis and imaging of bone quality (FTIR)," *Morphologie* **102**, 69–77 (2018).
35. T. J. Gal, T. Munoz-Antonia, C. A. Muro-Cacho, D. W. Klotch, "Radiation effects on osteoblasts *in vitro*: A potential role in osteoradionecrosis," *Arch. Otolaryngol. Head Neck Surg.* **126**, 1124–1128 (2000).
36. K. H. Szymczyk, I. M. Shapiro, C. S. Adams, "Ionizing radiation sensitizes bone cells to apoptosis," *Bone* **34**, 148–156 (2004).
37. B. Gong, M. E. Oest, K. A. Mann, T. A. Damron, M. D. Morris, "Raman spectroscopy demonstrates prolonged alteration of bone chemical composition following extremity localized irradiation," *Bone* **57**, 252–258 (2013).

38. B. R. Chrcanovic, P. Reher, A. A. Sousa, M. Harris, "Osteoradionecrosis of the jaws — a current overview — part 1: Physiopathology and risk and predisposing factors," *Oral Maxillofac. Surg.* **14**, 3–16 (2010).
39. D. R. Young, P. Virolainen, N. Inoue, F. J. Frassica, E. Y. Chao, "The short-term effects of cisplatin chemotherapy on bone turnover," *J. Bone Miner. Res.* **12**, 1874–1882 (1997).
40. M. J. Turunen, S. Saarakkala, H. J. Helminen, J. S. Jurvelin, H. Isaksson, "Age-related changes in organization and content of the collagen matrix in rabbit cortical bone," *J. Orthop. Res.* **30**, 435–442 (2012).
41. N. Pleshko, A. Boskey, R. Mendelsohn, "Novel infrared spectroscopic method for the determination of crystallinity of hydroxyapatite minerals," *Biophys. J.* **60**, 786–793 (1991).
42. C. Marcott, R. C. Reeder, E. P. Paschalis, D. N. Tatakis, A. L. Boskey, R. Mendelsohn, "Infrared microspectroscopic imaging of biomineralized tissues using a mercury-cadmium-telluride focal-plane array detector," *Cell Mol. Biol. (Noisy-le-grand)* **44**, 109–115 (1998).
43. E. Durchschlag, E. P. Paschalis, R. Zoehrer, P. Roschger, P. Fratzl, R. Recker, R. Phipps, K. Klaushofer, "Bone material properties in trabecular bone from human iliac crest biopsies after 3- and 5-year treatment with risedronate," *J. Bone Miner. Res.* **21**, 1581–1590 (2006).
44. H. W. Courtland, P. Nasser, A. B. Goldstone, L. Spevak, A. L. Boskey, K. J. Jepsen, "Fourier transform infrared imaging microspectroscopy and tissue-level mechanical testing reveal intraspecies variation in mouse bone mineral and matrix composition," *Calcif. Tissue Int.* **83**, 342–353 (2008).
45. M. J. Turunen, S. Saarakkala, L. Rieppo, H. J. Helminen, J. S. Jurvelin, H. Isaksson, "Comparison between infrared and Raman spectroscopic analysis of maturing rabbit cortical bone," *Appl. Spectrosc.* **65**, 595–603 (2011).
46. D. Farlay, Y. Bala, S. Rizzo, S. Bare, J. M. Lappe, R. Recker, G. Boivin, "Bone remodeling and bone matrix quality before and after menopause in healthy women," *Bone* **128**, 115030 (2019).
47. M. J. Turunen, V. Prantner, J. S. Jurvelin, H. Kröger, H. Isaksson, "Composition and microarchitecture of human trabecular bone change with age and differ between anatomical locations," *Bone* **54**, 118–125 (2013).
48. D. B. Burr, "Changes in bone matrix properties with aging," *Bone* **120**, 85–93 (2019).